

# Thermal Rectification and Negative Differential Thermal Resistance in a driven two segment classical Heisenberg chain

Debarshee Bagchi\*

*Theoretical Condensed Matter Physics Division,  
Saha Institute of Nuclear Physics, Kolkata, India.*

(Dated: March 24, 2018)

We investigate thermal transport in a two segment classical Heisenberg spin chain with nearest neighbor interaction and in presence of external magnetic field. The system is thermally driven by heat baths attached at the two ends and transport properties are studied using an energy conserving dynamics. We demonstrate that by properly tuning the bulk and interface parameters thermal rectification can be achieved - the system behaves as a good conductor of heat along one direction but becomes a bad conductor when the thermal gradient is reversed. Moreover, tuning the system parameters suitably gives rise to an interesting and technologically important feature known as the negative differential thermal resistance. The underlying physical mechanism responsible for the emergence of these features is explored.

## I. INTRODUCTION

Thermal management in low dimensional mesoscopic systems is an active topic of research at present. The quest to manipulate and control heat current, just as one can do with electrical current in electronic devices, has given birth to an altogether new branch of study, namely, the *phononics* [1, 2]. Needless to say, these studies are important not only in understanding the principles of low dimensional thermal transport, for example, necessary and sufficient condition for Fourier law [3–5], but also have immense technological application in today's world. Phononics deals with the manipulation of thermally excited phonons in the system and is now quite a mature field of research. Designs for many useful thermal devices have been proposed in recent times such as the thermal rectifier [6, 7], transistor [8], logic gates [9], memory elements [10], current limiter and constant current source [11]. In fact, very recently a thermal rectifier [12] and a thermal wave guide [13], both using carbon and boron nitride nanotubes, have been successfully fabricated in the laboratory. Apart from phonons, spin waves (magnons) in magnetic systems are also known to be an efficient carrier of energy transport for quite some time now [14]. Although considerable progress has been achieved in understanding magnon assisted thermal transport [15], a lot of effort still needs to be devoted before this can be utilized in real thermal devices.

The Heisenberg model [16, 17] is a paradigmatic model for magnetic insulators. Thermal transport properties of the one dimensional classical Heisenberg model have been studied in recent times and it is now known that in the thermodynamic limit heat transport in this model obeys Fourier law (diffusive transport of energy) for all temperature and magnetic field [18, 19]. This diffusive energy transport is attributed to the nonlinear spin wave interactions in this model which cause spin waves to scatter

[18]. However, for finite systems there can be a crossover from ballistic to diffusive behavior which crucially depends on the temperature [19] and also on other system parameters such as an external magnetic field. This is due to the fact that at very low temperature or very high magnetic field the entire system becomes correlated and heat energy can pass from the hotter to the colder end without being scattered.

In this paper we study the thermal transport in a two segment classical Heisenberg spin chain. The two segments are connected to each other by a link and external magnetic fields act on the spins in the chain. The spin spin coupling strengths and the magnetic fields can, in general, be different in the two segments but is the same for all spins belonging to one segment. Heat baths are attached to the two ends of the system and an energy current flows through the bulk of the system in response to the imposed thermal gradient. It is found that the thermal current can be rectified by suitably tuning the system parameters. Thus heat current can preferentially flow through the system along one direction while it is inhibited in the opposite direction i.e., when the thermal gradient is reversed.

Over the last decade, thermal rectification has been intensively investigated in a large number of theoretical as well as experimental works and in a variety of systems; for a recent review see [20]. Thermal rectification has been observed in many classical nonlinear asymmetric lattices in one dimension with different forms of interaction potentials e.g., Morse [6, 21], FK [7, 22], FK-FPU [23], graded mass harmonic systems [24, 25] to name a few. Studies of thermal rectification in two [26] and three [27] dimensions have also been done recently.

Another counterintuitive feature that emerges in some of these systems is the negative differential thermal resistance (NDTR) [7]. In the NDTR regime thermal current through a driven system is found to decrease as the imposed thermal gradient is increased. Although a lot of work [28–32] has been done to figure out the criteria responsible for the origin of NDTR, a comprehensive understanding is still lacking. This is however highly de-

---

\* E-mail address: debarshee.bagchi@saha.ac.in

sirable now, since NDTR is a promising feature and is believed to be crucial in the functioning of thermal devices, such as thermal transistors and thermal logic gates [8, 9].

In this paper we focus particularly on these two features - thermal rectification and negative differential thermal resistance. Rectification and NDTR have been previously studied in some detail for the two dimensional Ising spin system [33]. However there are certain differences between the Ising system and our chosen spin model. Firstly, Ising model is a discrete spin model and, although simple, it is not very realistic. A more realistic spin model is the Heisenberg model with continuous spin degree of freedom. Secondly, the 2d Ising model has a phase transition at a finite temperature whereas, the 1d Heisenberg model does not have a phase transition at any finite temperature. However thermal transport is found to be diffusive (obeys Fourier law) for both the models. Since an exact analytical treatment is generally not possible for most of the models mentioned above, an effective alternative is to investigate different generic models using numerical simulation. In the present work, we undertake such a numerical study of the above-mentioned features in a driven two segment classical Heisenberg spin system.

The organization of the paper is as follows. We define the two segment classical Heisenberg spin chain in detail in Sec. II. The simulation of the model has been performed using the discrete time odd even (DTOE) dynamics. The numerical implementation of this dynamics is briefly discussed in Sec. III. Thereafter in Sec. IV, we present our numerical results and demonstrate the existence of thermal rectification and negative differential thermal resistance in this system. We study dependencies of system parameters on these features and also investigate the necessary and sufficient conditions for the emergence of the NDTR regime. Finally, we conclude by summarizing our main results in Sec. V.

## II. MODEL

A schematic diagram of the model studied here is shown in Fig. 1. Consider two one-dimensional segments of spins connected to each other by a link. The spins  $\vec{S}_i^L$  ( $\vec{S}_i^R$ ) are conventional classical Heisenberg spins belonging to the left (right) segment of the chain and  $i$  is the site index which runs from  $1 \leq i \leq N_L$  ( $N_R$ ). Each spin on the left (right) segment interacts with an external magnetic field  $\vec{h}_L$  ( $\vec{h}_R$ ) which is taken to be the same for all spins in a particular segment. The Hamiltonian of the system is given as,

$$\mathcal{H} = \mathcal{H}_L + \mathcal{H}_I + \mathcal{H}_R \quad (1)$$

and the interaction of the spins in the left and the right segments are

$$\begin{aligned} \mathcal{H}_L &= -K_L \sum_{i=1}^{N_L} \vec{S}_i^L \cdot \vec{S}_{i+1}^L - \sum_{i=1}^{N_L} \vec{h}_L \cdot \vec{S}_i^L \\ \mathcal{H}_R &= -K_R \sum_{i=1}^{N_R} \vec{S}_i^R \cdot \vec{S}_{i+1}^R - \sum_{i=1}^{N_R} \vec{h}_R \cdot \vec{S}_i^R, \end{aligned} \quad (2)$$

where the  $K$ 's are the interaction strengths which is ferromagnetic for coupling  $K > 0$  and anti-ferromagnetic for  $K < 0$ . The interaction of the last spin of the left segment  $i = N_L$  and the first spin of the right segment  $i = 1$  is chosen to be of the form,

$$\mathcal{H}_I = -K_I [\lambda (S_i^x S_j^x + S_i^y S_j^y) + S_i^z S_j^z], \quad (3)$$

where  $\vec{S}_i = \vec{S}_{N_L}^L$  and  $\vec{S}_j = \vec{S}_1^R$  which defines the link connecting the two segments. For  $\lambda = 1$ , we refer to the interaction at the interface as the ‘‘Heisenberg’’ type, whereas, for  $\lambda = 0$ , the ‘‘Ising’’ type. For intermediate values of  $\lambda$  we have a ‘‘XXZ’’ type interaction at the interface.

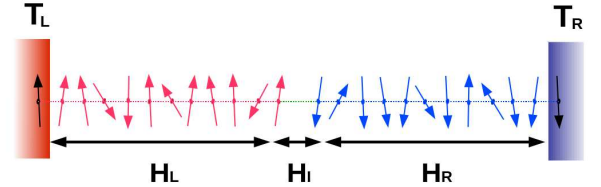


FIG. 1. (Color online) Schematic diagram of the two segment model.

The evolution equation for the spin vectors in the two segments can be written as,

$$\frac{d}{dt} \vec{S}_i = \vec{S}_i \times \vec{B}_i, \quad (4)$$

where  $\vec{B}_i = (K_i^- \vec{S}_{i-1} + K_i^+ \vec{S}_{i+1}) + \vec{h}_i$  is the local molecular field experienced by the spin  $\vec{S}_i$ ;  $K_i^-$  and  $K_i^+$  are the interactions of  $\vec{S}_i$  with  $\vec{S}_{i-1}$  and  $\vec{S}_{i+1}$  respectively and will be  $K_L$ ,  $K_R$  or  $K_I$  depending on the segment in which the spins  $\vec{S}_{i-1}$ ,  $\vec{S}_i$  and  $\vec{S}_{i+1}$  belong to. The magnetic field  $\vec{h}$  is equal to  $\vec{h}_L$  ( $\vec{h}_R$ ) for any spin  $\vec{S}_i$  belonging to the left (right) segment. For the two spins at the interface the equation of motion can be written down analogously.

This two segment system is thermally driven by two heat baths attached to the two ends. This is numerically implemented by introducing two additional spins at sites  $i = 0$  on the left segment and  $i = N_R + 1$  on the right segment. The bonds between the pairs of spins  $(\vec{S}_0^L, \vec{S}_1^L)$  and  $(\vec{S}_{N_R}^R, \vec{S}_{N_R+1}^R)$  at two ends of the system behave as stochastic thermal baths. The interaction strength of the bath spins with the system is taken to be

$K_b$ , and therefore energy of both the baths is bounded in the range  $(-K_b, K_b)$  and has a Boltzmann distribution. Thus the left and right baths are in equilibrium at their respective temperatures,  $T_L$  and  $T_R$  with average energies  $E_L = -K_b \mathcal{L}(K_b/T_L)$  and  $E_R = -K_b \mathcal{L}(K_b/T_R)$ ,  $\mathcal{L}(x)$  being the standard Langevin function. Thus one can set the two baths at a fixed average energies (or fixed temperatures) and an energy current flows through the system if  $T_L \neq T_R$ . In the steady state a uniform current (independent of the site index  $i$ ) transports energy from the hotter to the colder end of this composite system.

### III. NUMERICAL SCHEME

We investigate transport properties of the Heisenberg model by numerically computing the steady state quantities, such as, currents, energy profiles etc. using the energy conserving DTOE dynamics [19]. The DTOE dynamics updates spins belonging to the odd and even sublattices alternately using a spin precessional dynamics

$$\vec{S}_{i,t+1} = \left[ \vec{S} \cos \phi + (\vec{S} \times \hat{B}) \sin \phi + (\vec{S} \cdot \hat{B}) \hat{B} (1 - \cos \phi) \right]_{i,t}, \quad (5)$$

where  $\hat{B}_i = \vec{B}_i/|\vec{B}_i|$ ,  $\phi_i = |\vec{B}_i| \Delta t$  and  $\Delta t$  is the integration time step. The above formula is sometimes referred to as the *rotation formula* and holds for any finite rotation [34]. Note that Eq. 5 reduces to the equation of motion Eq. 4 in the limit  $\Delta t \rightarrow 0$ . The bath spins are refreshed by drawing the bond energies between the spins  $(\vec{S}_0^L, \vec{S}_1^L)$  and  $(\vec{S}_{N_R}^R, \vec{S}_{N_R+1}^R)$  from their respective Boltzmann distribution consistent with the temperature of the left and right bath temperatures. The left bath (at  $i = 0$ ) is updated along with the even spins and the right bath is updated along with the even or odd spins depending on whether  $i = N_R + 1$  is even or odd.

The DTOE dynamics alternately updates only half of the spins (odd or even) but all the bond energies are updated simultaneously. So the energy of the  $i$ -th bond  $\varepsilon_i^o$  measured immediately after the update of odd spins is not equal to its bond energy  $\varepsilon_i^e$  measured after the subsequent update of even spins, where we define the energy density  $\varepsilon_i = -\vec{S}_i \cdot [\vec{S}_i^+ \vec{S}_{i+1} + \vec{h}_i]$ . The difference  $\varepsilon_i^e - \varepsilon_i^o$  is the measure of the heat energy passing through the  $i$ -th bond in time  $\Delta t$ . Therefore the current  $J$  (rate of flow of energy) in the steady state is given by

$$J = \langle \varepsilon_i^e - \varepsilon_i^o \rangle / \Delta t. \quad (6)$$

Note that Eq. (6) can be shown to be consistent with the definition of current obtained using the continuity equation [19]. Numerically however, the current  $J$  can be computed as

$$J = -K_i^+ \langle (\vec{S}_i \cdot \vec{S}_{i+1})^e \rangle - \langle (\vec{S}_i \cdot \vec{S}_{i+1})^o \rangle / \Delta t, \quad (7)$$

since the magnetic field term cancels out in the above expression. The energy profile  $E_i$  for bulk sites in the two segments is computed as

$$E_i = - \left\langle \frac{1}{2} \vec{S}_i \cdot (K_i^- \vec{S}_{i-1} + K_i^+ \vec{S}_{i+1}) + \vec{h}_i \cdot \vec{S}_i \right\rangle, \quad (8)$$

For the left and the right boundaries (bath sites) energy is calculated as,

$$E_L = -K_b \langle \vec{S}_0^L \cdot \vec{S}_1^L \rangle \quad E_R = -K_b \langle \vec{S}_{N_R}^R \cdot \vec{S}_{N_R+1}^R \rangle. \quad (9)$$

A thorough discussion of the DTOE scheme in presence of thermal baths and its numerical implementation for the classical Heisenberg model can be found in Ref. [19]. In the following, we present our numerical results obtained using the DTOE dynamics for the two segment classical Heisenberg model.

### IV. NUMERICAL RESULTS

We study the two segment system with boundary temperatures  $T_L = T_0(1 + \Delta)$  and  $T_R = T_0(1 - \Delta)$ ; the average temperature of the system can be taken as  $\frac{1}{2}(T_L + T_R) = T_0$ . We set the segment sizes  $N_L = N_R = N$ , and the parameters are set as  $K_b = K_L = 1$ ,  $K_R = K$ ,  $\vec{h}_L = (0, 0, 1)$   $\vec{h}_R = (0, 0, h)$ . Thus the parameters we can manipulate reduce to  $\Delta, K, h$  and the interface parameters  $(K_I, \lambda)$ , all of which are kept restricted in the range  $(0, 1)$  unless mentioned otherwise. The time step  $\Delta t$  is chosen relatively larger since a larger  $\Delta t$  ensures faster equilibration of the system and because energy conservation is maintained for any finite  $\Delta t$  [19]. Also it can be shown that the final stationary state is the same for all choices of  $\Delta t$  [19]. In the following we set  $\Delta t = 2.0$  for all our simulations. Starting from a random initial configuration we evolve the spins using the DTOE dynamics. Once a nonequilibrium stationary state is reached, we compute various quantities, such as, the thermal current and the energy profiles for different values of the above mentioned parameters, temperature and system size.

#### A. Thermal rectification

First, we consider the system with  $\lambda = 1$  ("Heisenberg" type interaction at the interface) and study the thermal current through the system for different values of the parameter  $-1 < \Delta < 1$ . A positive  $\Delta$  implies that  $T_L > T_R$ , whereas, the same  $\Delta$  with a negative sign implies that the heat baths have been swapped between the two ends. We refer to  $\Delta > 0$  as the forward bias and  $\Delta < 0$  as the backward bias. Thus the entire system is now a Heisenberg spin chain with spatial asymmetry due to dissimilar spin-spin coupling strengths and magnetic fields in the two segments. The variation of the thermal current with the bias  $\Delta$  for different values of average

temperature  $T_0$  is shown in Fig. 2. We find that the thermal current is considerably larger for  $\Delta > 0$  whereas, for the same value of  $\Delta$  but with the baths interchanged, the current through the system is smaller. Thus, this nonlinear asymmetric two segment system behaves as a thermal rectifier i.e., it acts as a good conductor of heat in one direction and as a bad conductor in the reverse direction. This rectification effect is evidently more pronounced at lower temperatures as can be seen in Fig. 2.

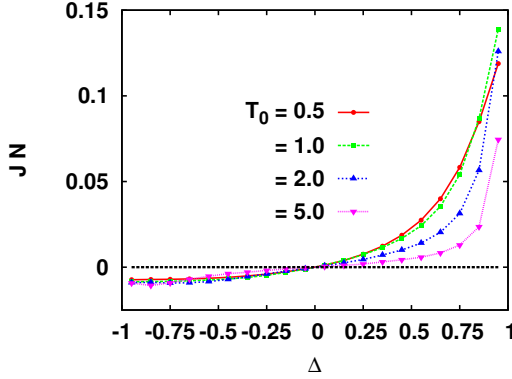


FIG. 2. (Color online) Variation of the thermal current  $J$  with  $\Delta$  for different average temperatures  $T_0$ . The parameters used are  $K = 0.5$ ,  $K_I = 0.05$ ,  $h = 0.1$  and segment size  $N = 100$ .

The steady state energy profiles of this two segment system is displayed in Fig. 3. for  $\Delta = 0.5$  and  $-0.5$ . It can be seen that the energy profile is almost flat implying that the system is near the ballistic regime, and there is an energy jump at the interface. This energy discontinuity is due to the interface thermal resistance, often referred to as the *Kapitza resistance* [35]. The current that flows in the system depends essentially on two factors, namely, the imposed bias and the interface resistance. The current increases as the bias is increased but decreases if the interface resistance is high which diminishes the current carrying capacity of the lattice i.e., its conductivity drops. It can be seen from Fig. 3 that the Kapitza resistance is comparatively larger for  $\Delta = -0.5$  than for  $\Delta = 0.5$ . This disparity in the interface resistance along the forward and the backward direction for the same bias magnitude  $\Delta$  results in the rectification of the thermal current. Thus in such nonlinear systems, the interface resistance is a function of the imposed driving field and has unequal values in the forward and the backward direction due to the spatial asymmetry of the lattice.

To quantify the amount of rectification, we compute the rectification efficiency defined as  $\eta = |J_+/J_-|$  where both the forward and the backward currents,  $J_+$  and  $J_-$ , are computed for the same  $|\Delta|$ . The variation of the rectification efficiency for  $|\Delta| = 0.5$  is shown in Fig. 4 for different values of average temperature  $T_0$ , magnetic field  $h$ , interface coupling  $K_I$  and segment size  $N$ . The rectification is found to decrease as the temperature, interface coupling strength and the system size increases.

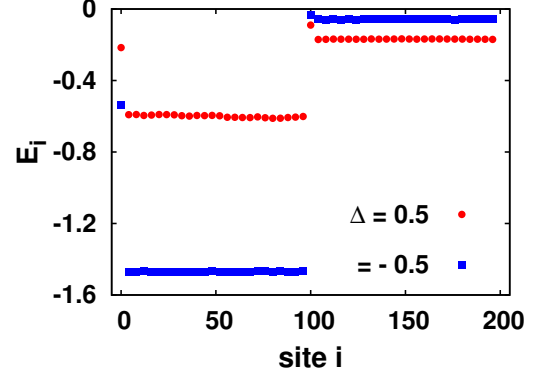


FIG. 3. (Color online) Energy profile of the system with  $\lambda = 1$  for positive  $\Delta = 0.5$  and negative  $\Delta = -0.5$  and parameters  $K = 0.5$ ,  $K_I = 0.05$ ,  $T_0 = 1.0$ ,  $h = 0.1$  and segment size  $N = 100$ .

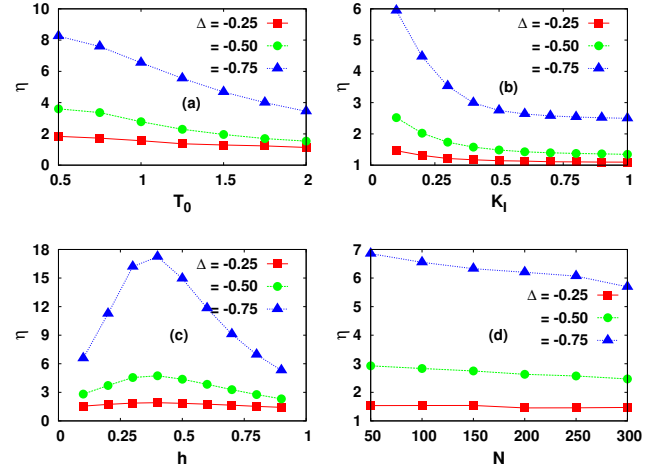


FIG. 4. (Color online) The variation of rectification efficiency  $\eta$  with (a) average temperature  $T_0$  (b) interface coupling  $K_I$  (c) magnetic field strength  $h$  and (d) segment size  $N$  is shown for  $\Delta = -0.25, -0.5$ , and  $-0.75$ . The values of the parameters are chosen as  $T_0 = 1.0$ ,  $K_I = 0.05$ ,  $h = 0.1$ ,  $K = 0.5$  and  $N = 100$ . In each plot only one of the above parameters is varied keeping all other values the same.

With magnetic field, the efficiency has a non-monotonic dependence in the range  $0 < h < 1$ . It first increases and attains a maximum value and decreases thereafter for larger  $h$  values close to unity. From the temperature and the system size data it is clear that rectification is more when the system is closer to the ballistic regime (lower temperature and smaller system size). As the magnetic field increases from zero, the system moves closer to the ballistic regime and thus efficiency  $\eta$  increases. However, as  $h$  approaches unity, there is a drop in the efficiency since the asymmetry of the system is gradually lost. Thus the non-monotonicity of the  $\eta \sim h$  curve is related to this interplay between ballistic/diffusive transport and asymmetry of the lattice. The efficiency attains a maximum value when both these factors have an optimum value.



If  $h$  is increased beyond unity the rectification will again start to increase due to spatial asymmetry. Since here rectification can be controlled externally by tuning the magnetic fields, one can achieve quite large rectification efficiency in this system.

### B. Thermal rectification and NDTR

Next, we set the parameter  $\lambda = 0$  and therefore now there is an “Ising” type interaction at the interface of the two segments. We study the transport properties as above and plot the thermal current  $J$  for different values of the parameter  $\Delta$ . The result obtained from simulation is displayed in Fig. 5. The rectification feature is also found in this case as above - the forward current (for  $\Delta > 0$ ) is appreciably larger in magnitude than the backward current (for  $\Delta < 0$ ).

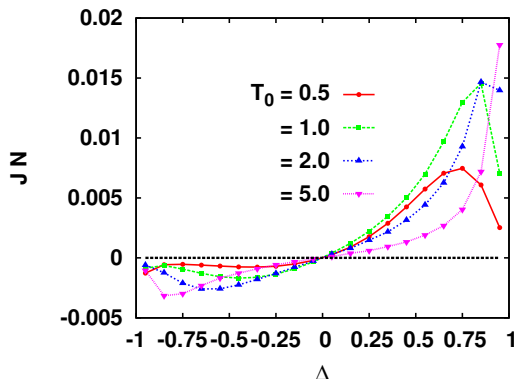


FIG. 5. (Color online) Variation of the thermal current  $J$  with  $\Delta$  for different average temperatures  $T_0$ . The parameters used are  $K = 0.5$ ,  $K_I = 0.05$ ,  $h = 0.1$  and segment size  $N = 100$ .

In addition, careful observation reveals that for certain regions of the  $J \sim \Delta$  curves, the current actually decreases as  $|\Delta|$  is increased. Thus unlike the case of  $\lambda = 1$ , where the magnitude current  $J$  is a strictly non-decreasing function of the parameter  $\Delta$ , for  $\lambda = 0$  it is a non-monotonic function. This feature can be seen in certain ranges for all the four  $J \sim \Delta$  curves shown in Fig. 5. This is known as the *negative differential thermal resistance* (NDTR). The emergence of the NDTR regime is not dependent on the asymmetry of the lattice; we will show that a purely symmetric lattice also exhibits the NDTR feature. The generic parameter dependencies of the rectification efficiency will be roughly the same as that of the previous case and can be analyzed similarly, except that the current here is a non-monotonic function of the gradient which has to be taken into account. This nonmonotonicity can be exploited to achieve a higher rectification efficiency by choosing the parameters in the two segments properly. In the following, we focus only on the NDTR feature and try to understand the factors influencing the emergence of the NDTR region.

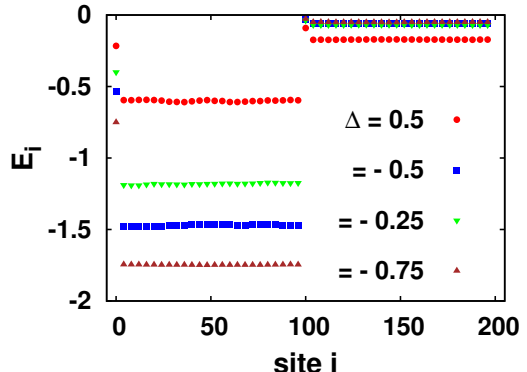


FIG. 6. (Color online) Energy profile of the system with  $\lambda = 0$  for positive  $\Delta = 0.5$  and negative  $\Delta = -0.25, -0.5, -0.75$  for  $K = 0.5$ ,  $K_I = 0.05$ ,  $T_0 = 1.0$ ,  $h = 0.1$  and  $N = 100$ .

The energy profiles for different values of  $\Delta$  is shown in Fig. 6. The rectification effect here can be again explained by noting that the Kapitza resistance is larger for the backward bias, similar to the previous case. The occurrence of the NDTR is a consequence of the non-linear response of the lattice which causes the interface resistance to behave nonlinearly for larger thermal gradients. The current increases regularly as the gradient increases but the interface resistance also increases and the current conductivity of the lattice decreases. When the decrease in the current due to the interface resistance dominates the increases in current due to the imposed gradient NDTR emerges in such two segment nonlinear systems [28].

We focus on the  $\Delta < 0$  region of the  $J \sim \Delta$  curve and first study the parameter dependencies of the NDTR feature. Since it is difficult to compare NDTR regimes for different parameters and system sizes directly (because the current has different typical values), we define a quantity  $\gamma \equiv (J_{m+1} - J_m)/J_m$  which is essentially the change in the thermal current scaled by the typical value of the current, for two consecutive discrete values of  $\Delta$  belonging to  $\{\Delta_m\}$  where  $1 \leq m \leq M$ ,  $M$  being the total number of  $\Delta$  values for which the current has been numerically computed. Note that if  $|\Delta_{m+1}| > |\Delta_m|$  then  $\gamma$  is positive for positive differential thermal resistance (PDTR) and negative in the NDTR regime. Thus  $\gamma$  indicates the onset and also the width of the NDTR regime.

In Fig. 7 we show the quantity  $\gamma$  with  $\Delta$  for different parameters  $T_0$ ,  $h$ ,  $K_I$  and size  $N$ . We find that the NDTR regime sets in for smaller  $\Delta$  values at lower average temperature  $T_0$  and the NDTR region vanishes as  $T_0$  is increased. It is also found that that NDTR is more pronounced for smaller values of the interface coupling  $K_I$ . With system size the NDTR regime remains unaffected which is strikingly different from the result obtained for generic nonlinear models where the NDTR regime vanishes for larger sizes [28]. Thus for a wide range of segment sizes (which differ by an order of magnitude, see Fig. 7b) the onset of NDTR occurs at the same value

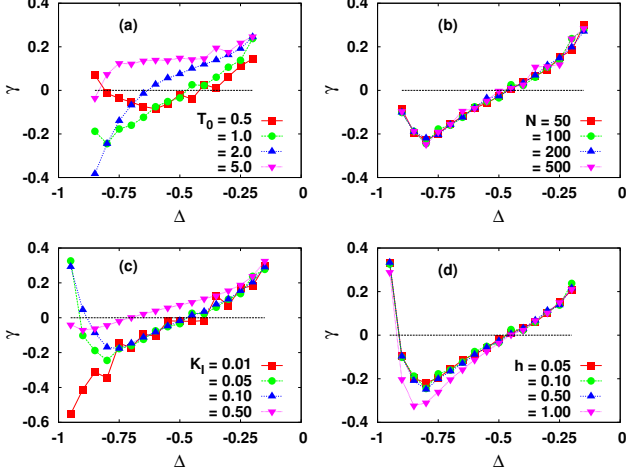


FIG. 7. (Color online) Variation of  $\gamma$  with  $\Delta$  for different (a) average temperature  $T_0$  (b) segment size  $N$  (c) interface coupling  $K_I$  and (d) magnetic field strength  $h$ . The values of the parameters are set as  $K = 0.5$ ,  $T_0 = 1.0$ ,  $K_I = 0.05$ ,  $h = 0.1$ , and  $N = 100$ , and only one of the parameters is varied in each of the above plots.

of  $\Delta$  and there is no noticeable difference in the onset or the width of the NDTR region. This size independence of the NDTR region in this system is due to the fact that the lattice is very close to the ballistic regime where the thermal current is independent of the system size. The onset of the NDTR phase for different values of the magnetic field occurs at the same value of  $\Delta$ ; for larger fields the magnitude of resistance seems to be slightly larger.

It has been suggested in as previous work [29] that the appearance of the NDTR is related to ballistic heat transport processes in the lattice. Thus a PDTR to NDTR transition occurs when there is an accompanying crossover from diffusive to ballistic transport of heat energy in the system. We find that ballistic transport is indeed a necessary condition for the appearance of NDTR in this model. The supporting numerical evidence is presented in Fig. 8. For the  $\lambda = 0$  system, transport can be made to be diffusive by choosing the parameters properly, but then the NDTR region ceases to exist and emerges only for ballistic transport. Thus it appears that ballistic transport of energy in a system is a necessary criterion for NDTR to exist. However this is not a sufficient condition as has been shown for the Morse lattice [30] where a PDTR to NDTR transition occurs without any accompanying diffusive to ballistic crossover. For our model with  $\lambda = 1$ , a diffusive to ballistic transport can also occur as the system parameters are changed but this system always exhibits PDTR as can be seen in Fig. 8.

For intermediate values of  $\lambda$  in the range  $0 < \lambda < 1$  the simulation results are presented in Fig. 9. We find that for smaller  $\lambda$  values, the NDTR regime appears in the  $J \sim \Delta$  curve whereas for larger values it vanishes. Evidently, a smaller  $\lambda$  implies lesser nonlinearity of the interface coupling and thus the NDTR regime is more pro-

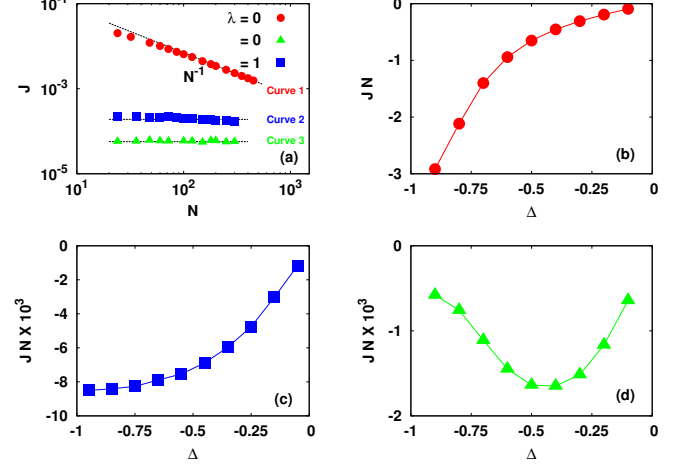


FIG. 8. (Color online) (a) The variation of the thermal current with system size is shown for the following cases (i) Curve 1: for  $\lambda = 0$ , the system is in the diffusive regime for parameters  $K = 1.0$   $K_I = 1.0$  and no magnetic field, and does not show NDTR as shown in (b); (ii) Curve 2: for  $\lambda = 1$ , the system in the ballistic regime for parameters  $K = 0.5$   $K_I = 0.05$   $h = 0.10$  and does not show NDTR as shown in (c); (iii) Curve 3: for  $\lambda = 0$ , the system is in the ballistic regime for parameters  $K = 0.5$   $K_I = 0.05$   $h = 0.10$  and shows NDTR as shown in (d). Average temperature for all the curves is  $T_0 = 1.0$ .

nounced. This has also been observed in generic phononic systems that the NDTR regime actually diminishes and eventually vanishes as nonlinearity is added to the link interaction [31]. Thus for the occurrence of NDTR the two segments should have a higher degree of nonlinearity as compared to that of the link interaction. Also note that the lattice has no spatial asymmetry (see Fig. 9) and yet exhibits NDTR which clearly shows that asymmetry is not an essential criterion for the emergence of NDTR.

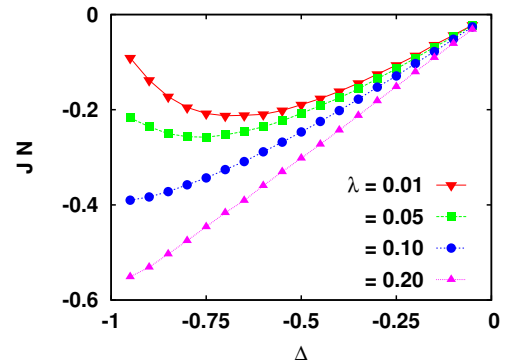


FIG. 9. (Color online) The variation of thermal current with  $\Delta$  in a spatially symmetric lattice for different values of  $\lambda$ . The parameters chosen are  $K = 1.0$ ,  $T_0 = 1.0$ ,  $h = 1.0$  and segment size  $N = 100$ . The NDTR regime shrinks as  $\lambda$  is increased.

## V. CONCLUSION

To summarize, we have performed extensive numerical simulation of a two segment thermally driven classical Heisenberg spin chain in presence of external magnetic field. The spin couplings and the applied magnetic fields can in general take different values in the left and the right segment. The composite system is thermally driven by attaching heat reservoirs at the two ends. By properly tuning the interface and bulk parameters one can achieve thermal rectification in this system. Thus the system behaves as a good conductor of thermal energy along one direction but restricts the flow of energy in the opposite direction. The rectification efficiency is found to be controlled by nonlinearity and spatial asymmetry of the lattice.

The rectification of thermal current in such nonlinear asymmetric two segment lattices can be physically interpreted in terms of the interface resistance which is found to be larger in one direction as compared to the other. The rectification efficiency drops as the system size or the average temperature is increased since a crossover occurs from ballistic to diffusive transport of energy. The rate of this decrease in efficiency is lower when the system is

closer to the ballistic regime and this can be controlled by tuning the external magnetic field accordingly. Thus deep inside the ballistic regime the efficiency is practically independent of the system size or the temperature.

Besides rectification, negative differential thermal resistance can also emerge in this system where the thermal current decreases as the imposed gradient is increased. The occurrence of NDTR is crucially dependent on the nonlinearity of the lattice and emerges in this system when there is a diffusive to ballistic crossover. One can choose the system parameters such that the NDTR regime becomes independent of the system size by maintaining the system in the ballistic regime. Also, NDTR can emerge without spatial asymmetry and therefore it is possible have thermal rectification without NDTR and vice versa. The NDTR region is pronounced at low temperature and for weak interface coupling and diminishes when nonlinearity is added to the link interaction. Hopefully, with the advancement of low dimensional experimental techniques these theoretical predictions can be verified and lead to the fabrication of devices for efficient thermal management.

**Acknowledgement:** The author would like to thank P. K. Mohanty for helpful suggestions and careful reading of the manuscript.

- 
- [1] N. Li, J. Ren, L. Wang, G. Zhang, P. Hänggi, B. Li, Rev. Mod. Phys. **84**, 1045-1066 (2012).
  - [2] G. Casati, Chaos **15**, 015120 (2005).
  - [3] F. Bonetto, J. L. Lebowitz, and L. Rey-Bellet, *Fourier law: A challenge to theorists*, in Mathematical Physics 2.
  - [4] S. Lepri, R. Livi, and A. Politi, Phys. Rep. **377**, 1 (2003).
  - [5] A. Dhar, Advances in Physics, **57**, 457, (2008).
  - [6] M. Terraneo, M. Peyrard, and G. Casati, Phys. Rev. Lett. **88**, 094302 (2002).
  - [7] B. Li, L. Wang, and G. Casati, Phys. Rev. Lett. **93**, 184301 (2004).
  - [8] B. Li, L. Wang, and G. Casati, Appl. Phys. Lett. **88**, 143501 (2006).
  - [9] L. Wang and B. Li, Phys. Rev. Lett. **99**, 177208 (2007).
  - [10] L. Wang and B. Li, Phys. Rev. Lett. **101**, 267203 (2008).
  - [11] J. Wu, L. Wang, and B. Li, Phys. Rev. E **85**, 061112 (2012).
  - [12] C. W. Chang, D. Okawa, A. Majumdar, and A. Zettl, Science **314**, 1121 (2006).
  - [13] C. W. Chang, D. Okawa, H. Garcia, A. Majumdar, and A. Zettl, Phys. Rev. Lett. **99**, 045901 (2007).
  - [14] H. Fröhlich, W. Heitler, Proc. Roy. Soc. (London) A155, 640 (1936).
  - [15] C. Hess, Eur. Phys. J. Special Topics **151**, 73 (2007); A. V. Sologubenko, T. Lorenz, H. R. Ott, and A. Freimuth, J. Low Temp. Phys. **147**, 387 (2007).
  - [16] M. E. Fisher, Am. J. Phys. **32**, 343 (1964).
  - [17] G. S. Joyce, Phys. Rev. **155**, 478 (1967).
  - [18] A. V. Savin, G. P. Tsironis, and X. Zotos, Phys. Rev. B **72**, 140402(R) (2005).
  - [19] D. Bagchi and P. K. Mohanty, Phys. Rev. B **86**, 214302 (2012).
  - [20] N. A. Roberts and D. G. Walker, Int. J. Thermal Sci. **50**, 648 (2011).
  - [21] B. Hu, D. He L. Yang and Y. Zhang, Phys. Rev. E **74**, 060101(R) (2006).
  - [22] B. Hu, L. Yang, and Y. Zhang, Phys. Rev. Lett. **97**, 124302 (2006).
  - [23] J. Lan, L. Wang, B. Li, Phys. Rev. Lett. **95**, 104302 (2005).
  - [24] N. Yang, N. Li, L. Wang, and B. Li, Phys. Rev. B **76**, 020301(R) (2007).
  - [25] J. Wang, E. Pereira and G. Casati, Phys. Rev. E **86**, 010101(R) (2012).
  - [26] J. Lan, B. Li, Phys. Rev. B **74**, 214305 (2006).
  - [27] J. Lan, B. Li, Phys. Rev. B **75**, 214302 (2007).
  - [28] D. He, S. Buyukdagli, and B. Hu, Phys. Rev. B **80**, 104302 (2009).
  - [29] W.-R. Zhong, P. Yang, B.-Q. Ai, Z.-G. Shao, and B. Hu, Phys. Rev. E **79**, 050103(R) (2009).
  - [30] Z.-G. Shao and L. Yang, EPL, **94**, 34004 (2011).
  - [31] Z.-G. Shao, L. Yang, \* H.-K. Chan, and B. Hu, Phys. Rev. E **79**, 061119 (2009).
  - [32] D. He, B.-q. Ai, H.-K. Chan, and B. Hu, Phys. Rev. E **81**, 041131 (2010).
  - [33] L. Wang and B. Li, Phys. Rev. E **83**, 061128 (2011).
  - [34] H. Goldstein, C. P. Poole and J. L. Safko, Classical Mechanics, 3rd Edition, Addison Wesley.
  - [35] E. T. Swartz and R. O. Pohl, Rev. Mod. Phys. **61**, 605 (1989).